Materials Research Express

PAPER

Defect properties of vanadium doped barium titanate ceramics

R Böttcher[1], H T Langhammer[2,4], T Walther[2], F Syrowatka[3] and S G Ebbinghaus[2]

[1] Fakultät für Physik und Geowissenschaften, Universität Leipzig, Linnéstraße 5, D-04103 Leipzig, Germany
[2] Institut für Chemie, Martin-Luther-Universität Halle-Wittenberg, Kurt-Mothes-Straße 2, D-06120 Halle (Saale), Germany
[3] Interdisziplinäres Zentrum für Materialwissenschaften, Martin-Luther-Universität Halle-Wittenberg, Heinrich-Damerow-Straße 4, D-06120 Halle (Saale), Germany
[4] Author to whom any correspondence should be addressed.

E-mail: boettch@physik.uni-leipzig.de, hans.langhammer@physik.uni-halle.de, till.walther@chemie.uni-halle.de, frank.syrowatka@cmat.uni-halle.de and stefan.ebbinghaus@chemie.uni-halle.de

Keywords: barium titanate, vanadium doped, defect chemistry, EPR, magnetic susceptibility

OPEN ACCESS

RECEIVED
15 July 2019

REVISED
16 August 2019

ACCEPTED FOR PUBLICATION
13 September 2019

PUBLISHED
11 October 2019

Abstract

X-ray diffraction (XRD) patterns, electron probe microanalysis (EPMA), electron paramagnetic resonance (EPR) powder spectra (9 and 34 GHz) and the magnetic susceptibility of $BaTiO_3 + 0.04\ BaO + 0.01\ V_2O_5$ ceramics were studied to investigate the valence states of V ions and their solubility in the $BaTiO_3$ lattice. In samples sintered at 1400 °C in air, only about 0.1 mol% V is incorporated in the $BaTiO_3$ lattice being in V^{4+} and V^{5+} valence state, respectively. 95% of the nominal V dopant content occurs in the secondary phase $Ba_3(V/Ti)_2O_8$. All $BaTiO_3$ samples investigated are in tetragonal phase at room temperature. In the as-sintered samples V^{4+} is detected at temperatures $T < 20$ K by its hyperfine structure (HFS) octet due to the nuclear spin 7/2 of ^{51}V. Samples post-annealed in H_2/Ar atmosphere at 1200 °C exhibit a further HFS octet occurring at $T > 25$ K and vanishing at $T > 250$ K, which is caused by V^{2+} ions. This spectrum is characterized by a simultaneous HFS and fine structure splitting constituted by allowed and forbidden transitions. Both V^{4+} and V^{2+} ions are incorporated at Ti^{4+} sites of the $BaTiO_3$ lattice.

1. Introduction

Barium titanate ($BaTiO_3$) is a material of fundamental importance for a wide range of technical applications (multi-layer ceramic capacitors, ferroelectric random access memories, piezoelectric sensors, actuators, etc) [1–3] and a model system of the theoretical description of ferroelectricity due to the variety of phase transitions. Besides the well-known, temperature-driven phase transitions

$$cubic \xrightarrow{125\ ^\circ C} tetragonal \xrightarrow{\approx 0\ ^\circ C} orthorhombic \xrightarrow{\approx -90\ ^\circ C} rhombohedral$$

of the 3 C modification $BaTiO_3$ shows a further structural phase transition into the hexagonal high temperature 6 H modification. This modification is stable at temperatures >1430 °C in air as far as undoped material is concerned. Extrinsic defects, particularly the 3d-, 4d-, 4f- and 5d-ions as well as vacancies, can change the physical properties of this material in a wide range. This distinct ability of tailoring of its physical properties is the basis of the numerous technical applications of $BaTiO_3$-based materials. In the past, extensive investigations (permittivity, electrical and thermal conductivity, electromechanical and optical properties, etc) were undertaken to probe in particular the influence of the 3d-ions on the macroscopic properties of barium titanate ceramics. On the other hand, optical and EPR investigations can provide complementary microscopic information on the 3d-ions incorporated in the $BaTiO_3$ matrix, as e.g. their charge, crystallographic site, and local symmetry of their surrounding.

In contrast to the dopants Cr, Mn, Fe, Co, Ni and Cu (see e.g. [4–11]), sparse information on the physical properties of V-doped $BaTiO_3$ is available in the literature. In 1971 Feltz *et al* [12] investigated V-doped $BaTiO_3$ single crystals grown by the flux method in reducing atmosphere. They reported a very low solubility of vanadium in the $BaTiO_3$ lattice with maximum 1.3 at% V^{4+} measured potentiometrically. Later several authors [13, 14] found no measureable paramagnetism in air-sintered V-doped $BaTiO_3$ ceramics. Schwartz *et al* [15]

found no significant EPR spectrum in 0.04 mol% V-doped $BaTiO_3$ ceramics sintered in air. Liu *et al* [16] investigated V-doped ceramics with V contents up to 2 mol% sintered in air and reported a solubility of less than 1 mol% V with a maximum sample density at 0.1 mol% V. Their samples are tetragonal at room temperature and exhibit distinct amounts of secondary phases, identified as $Ba_3V_2O_8$ and $BaVO_{2.8}$ by XRD. There are few investigations on the influence of vanadium on the dielectric properties and the microstructure of barium titanate and solid solutions with strontium titanate, barium zirconate and barium hafnate ceramics [16–21]. In the case of barium titanate, partially inconsistent data are reported on the shift direction of the Curie temperature and on the dielectric/ferroelectric data in general [17, 18]. Often it seems that the authors have not noticed the low solubility of vanadium in $BaTiO_3$ and additionally it is mostly assumed that vanadium is in the V^{5+} state without experimental evidence.

The first EPR measurement on V-doped $BaTiO_3$ ceramics annealed under strongly reducing conditions was made by Schwartz *et al* [15]. A complex spectrum with a hyperfine pattern spread over ≈650 G and centered around $g \approx 2$ was observed in X-band. The authors did not analyse the powder spectrum in detail but they suggest, based on the study of Müller *et al* on $SrTiO_3$:V [22] that the observed EPR specrum is most likely due to V^{2+}. Later, to the best of our knowledge, only Shibahara *et al* [23] reported on EPR investigations of V^{4+} in $BaTiO_3$-based ceramic multilayer capacitors without giving any details of the measurement. Unlike for $BaTiO_3$, there are several studies of vanadium-doped $SrTiO_3$ single crystals by Kool *et al* [24, 25] and Müller *et al* [22]. After illumination ($\lambda \approx 396$ nm), an intensive EPR spectrum was observed in this material and characterized as a $S = 1/2$ centre with tetragonal symmetry. On the basis of the hyperfine splittings the spectrum has been attributed to V^{4+} substituting for Ti^{4+} [24]. The strain-induced effects (by applied uniaxial stress) were interpreted assuming that the $SrTiO_3$:V^{4+} system has a threefold degenerated vibronic ground state. This vibronic degeneracy is derived from a strong Jahn-Teller effect [25]. After reducing treatment (heating in 6% H_2/N_2 atmosphere above 1200 °C and subsequent quenching) of $SrTiO_3$ single crystals containing 0.2 mol% vanadium, an EPR spectrum of V^{2+} ($3d^3$) with the electronic spin $S = 3/2$ was observed. The g-shift and the hyperfine splitting (HFS) of the central fine structure transition indicate a 40% delocalisation of the spin-density onto Ti conduction band levels. Upon cooling below 130 K the V^{2+} intensity decreases due to carrier freeze-out from V^{2+} to V^{3+}. An exponential line width narrowing is observed with activation energy of 200 meV, which can be accounted for by the thermally activated hopping between V^{2+} (double) and V^{3+} (single) acceptors [22].

In this paper we present first detailed EPR investigations and EPMA measurements of vanadium doped barium titanate ceramics to gain a deeper insight into the nature of the vanadium defect (incorporation site, valence state) and its solubility into the $BaTiO_3$ lattice for air-sintered material.

2. Experimental procedure

A pre-ceramic powder with the nominal composition $BaTiO_3 + 0.04\,BaO + 0.01\,V_2O_5$ was prepared by the conventional mixed-oxide powder technique. After mixing (agate balls, water) and calcining (1100 °C, 2 h) of $BaCO_3$ (Solvay, VL600, <0.1 mol % Sr), TiO_2 (Merck, no. 808) and V_2O_3 (Merck, p.a.), the obtained $BaTiO_3$ powder was fine-milled (agate balls, 2-propanole) and densified to disks with a diameter of 6 mm and a height of about 3 mm. These disks were sintered in air at a temperature of 1400 °C for one hour (heating rate 10 K min^{-1}). Afterwards, several of them were annealed in a stream of H_2/Ar (20/20 ml min^{-1}) at 1200 °C for 120 min.

X-ray powder diffraction on crushed samples was performed with a Bruker D8 Advance Bragg-Brentano diffractometer equipped with a one-dimensional silicon strip detector (LynxEye™) using Cu-K_α radiation. The angular range $5 \leqslant 2\theta \leqslant 60°$ was recorded with a step size of 0.0105° and a counting time of 1 s/step. The variable divergence slit was set to illuminate a constant area of $10 \times 6\,mm^2$.

Magnetic measurements were carried out using the ACMS magnetometer option of a PPMS 9 (Quantum Design). The temperature-dependent magnetic moments were measured at 9.0 T in the temperature range 5-300 K. The obtained magnetic moments were corrected for the magnetic moment of the sample holder and with respect to the magnetic contribution of the $BaTiO_3$ matrix.

The microstructure of polished and chemically etched specimens was examined by scanning electron microscopy (SEM) using a FEI (Thermofisher) VERSA 3D (Dual Beam FIB). The vanadium concentration within the $BaTiO_3$ grains was measured by wavelength-dispersive x-ray EPMA (WDX-EPMA, model CAMEBAX, Cameca), whereas the V-rich secondary phases inside the ceramics were analysed both with EDX system by EDAX attached to the VERSA 3D and with the CAMEBAX WDX system.

EPR measurements of pulverized ceramics were carried out in X- (9.4 GHz) and Q-band (34 GHz) with Bruker EMX devices. Temperatures between 5 and 240 K were achieved with Oxford flowing He gas cryostats in connection with an Oxford ITC controller (temperature stability about 0.2 K).

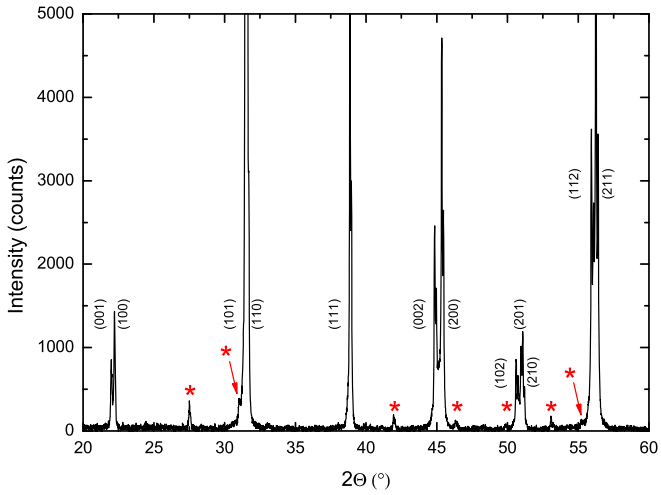

Figure 1. Room-temperature XRD pattern of crushed 2 mol% V doped as-sintered $BaTiO_3$ ceramics. Peaks with Miller-indices belong to tetragonal $BaTiO_3$ while the peaks marked by an asterisk correspond to $Ba_3V_2O_8$.

For the determination of the spin-Hamiltonian parameters and the evaluation of the powder EPR spectra the MATLAB[5] toolbox for electron paramagnetic resonance 'Easy Spin 5.2.11' was used [26]. Simulating powder spectra of the standard spin Hamiltonians

$$\hat{H} = \mu_B \vec{B} \underline{g} \hat{\vec{S}} + \hat{\vec{S}} \underline{A} \hat{\vec{I}} \tag{1}$$

for electron spin $S = 1/2$ systems (V^{4+} ions) and

$$\hat{H} = \mu_B \vec{B} \underline{g} \hat{\vec{S}} + D\left(\hat{S}_z^2 + \frac{1}{3}S(S+1)\right) + \hat{\vec{S}} \underline{A} \hat{\vec{I}} \tag{2}$$

for electron spin $S = 3/2$ systems (V^{2+} ions) a satisfactory accuracy in the determination of the respective parameters was achieved. The parameters are the components of the $\underline{g}$ tensor and of the hyperfine structure (HFS) tensor $\underline{A}$ of the nucleus of ^{51}V (abundance 100%) with $I = 7/2$ and the axial fine structure parameter D. $\vec{B}$ is the magnetic field, $\hat{\vec{S}}$ and $\hat{\vec{I}}$ are the electron and nuclear spin operators, respectively, and μ_B is the Bohr magneton. The spectrum of one defect species cannot be modelled by the same parameters $\underline{g}$, $\underline{A}$ and D for each grain of the ceramic powder samples since the local symmetry in the surrounding of the paramagnetic defect is weakly distorted by varying strain effects. Therefore, we used distributions of the principal values of the g tensor for the 1/2-spin system (V^{4+} ions). In the case of the 3/2-spin system only the distribution of the fine structure parameter D was considered. Assuming random fluctuations in the local lattice parameters in the vicinity of the paramagnetic impurity these distributions can be approximated by a Gaussian function with full widths at half-height (FWHH) $\Delta g_{||}, \Delta g_{\perp}$ and ΔD.

3. Results

3.1. XRD, microstructure and solubility of vanadium

Figure 1 shows the room temperature (RT) XRD pattern of an as-sintered sample with 2.0 mol% vanadium.

It consists of tetragonal $BaTiO_3$ and small traces of a V-containing secondary phase, which was identified as $Ba_3V_2O_8$. For a quantitative phase analysis a Rietveld refinement was carried out using the Fullprof program suite. The amount of $Ba_3V_2O_8$ accounted to 3 mass% corresponding to 1.1 mol%. The samples annealed in different atmospheres at different temperatures remain tetragonal at RT with one exception, namely the highly reducing treatment in H_2/Ar at 1400 °C for 10 hours. In these samples $BaTiO_3$ is completely in the hexagonal modification at RT and therefore they are not considered in this work.

An example of the microstructure of a polished and chemically etched as-sintered sample with 2.0 mol% vanadium is shown in figure 2.

Compared with undoped $BaTiO_3$ ceramics prepared under the same conditions and exhibiting a mean grain size of about 50 μm, the vanadium dopant reduces the grain size to values below 20 μm and increases the

[5] MATLAB is a registered trademark of the MathWorks, Inc., Natick, MA, USA.

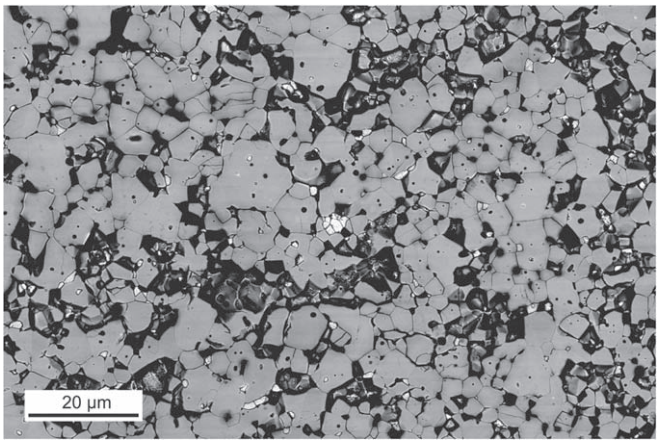

Figure 2. BSE image of the microstructure of 2 mol% V doped as-sintered $BaTiO_3$ ceramics. V doped $BaTiO_3$ grains appear grey colored while the much brighter grains correspond to the secondary phase identified as $Ba_3(V/Ti)_2O_8$. The nearly black regions are pores or holes.

porosity distinctly, as visible by the black areas corresponding to holes. On the other hand, we cannot exclude that a part of the holes visible in figure 2 may be caused by grains pulled out during the grinding/polishing process. Figure 2 was taken in back scattered electron (BSE) mode, thus the brightness reflects the mean atomic number of the grains. Therefore, the Ba-rich secondary phase $Ba_3V_2O_8$ can be well recognized by its white color in contrast to the grey $BaTiO_3$ grains. Because of the rather low solubility of vanadium in the $BaTiO_3$ lattice [12], WDX-EPMA investigations were performed to determine the V concentration inside the $BaTiO_3$ particles. Quantitative analysis of the vanadium concentration resulted in a value of 0.10 ± 0.01 mol%, which is the mean value of numerous measurements taken at different points in each of a large number of grains. Hence, 95% of the dopant in a sample doped with nominally 2.0 mol% V is actually incorporated in the secondary phase. A second sample with nominally 10 mol% V was also investigated. The mean value of the vanadium concentration in the grains amounted to 0.15 ± 0.01 mol%, i.e. a similar content as in the sample with a nominal concentration of 2 mol%. These results show that the solubility limit of vanadium in $BaTiO_3$ prepared in air can be estimated to $\leqslant 0.2$ mol%. Furthermore, we tried to quantify the V content of the V-rich phase by WDX. Unfortunately, the analysis of several grains gave no clear picture, most likely due to the large excitation volume of the x-ray, which is about 1.5 μm for 20 keV electrons and a sample density of 6 g cm^{-3} [27]. As a consequence, neighboring $BaTiO_3$ also contributes to the WDX signal. For this reason, EDX measurements with a lower electron acceleration voltage of 12 keV were performed with the EDAX system attached to the VERSA 3D FIB. They resulted in an atomic ratio Ba:(V + Ti) of nearly 3:2 in the majority of the V-rich grains investigated, confirming that the secondary phase is $Ba_3(V/Ti)_2O_8$. Obviously, the incorporated Ti atoms (V:Ti $\approx$ 3:2) change the position of the XRD peaks only slightly compared to pure $Ba_3V_2O_8$ (see figure 1).

3.2. Magnetic susceptibility

Figure 3 shows the molar magnetic susceptibility of an as-sintered sample doped with nominally 2.0 mol% vanadium measured in a magnetic field of 9.0 T.

At temperatures above ca. 220 K, the measured paramagnetic moment reaches the detection limit of the instrument. Therefore, we restricted the data evaluation to the low temperature region. The molar susceptibility was calculated based on the assumption that the paramagnetic behavior of the sample is caused by 0.1 mol% V. This is a rather rough estimation because of two reasons. First, a part of the vanadium incorporated in the $BaTiO_3$ grains could be in the diamagnetic V^{5+} valence state. Second, since the vanadium in the detected $Ba_3V_2O_8$ phase exhibits a mixed valence of +5 (majority) and +4 [28], the amount of paramagnetic V ions in the secondary phase cannot be neglected. Since the calculated value of n_{eff} close to 2.7 (figure 3) significantly depends on the uncertain molar paramagnetic susceptibility, it unfortunately cannot be used for a rough estimation of the electron configuration of the V ions by the spin-only approximation[6]. The interpretation of the susceptibility data is described in section 4 following the discussion of the EPR data.

[6] In the spin-only approximation, $n_{eff} = 2.8$ corresponds to S = 1 pointing to V^{3+} ions with two unpaired d electrons.

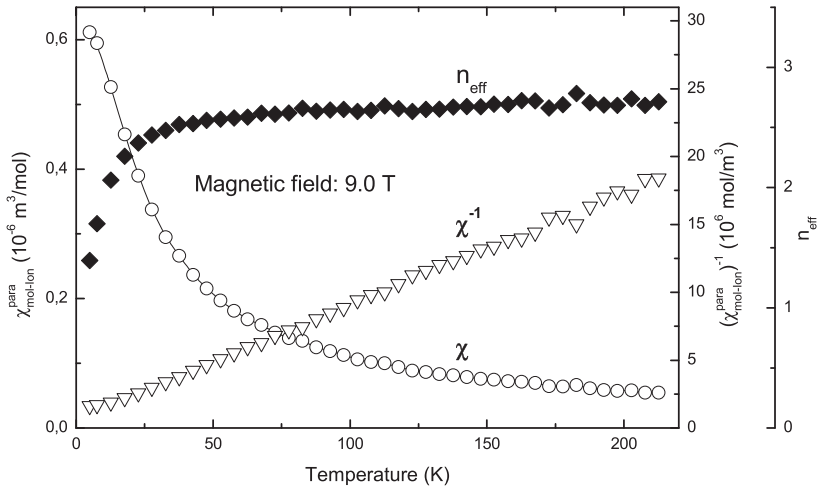

Figure 3. Molar magnetic susceptibility, reciprocal susceptibility and effective Bohr magneton number of 2 mol% V doped as-sintered $BaTiO_3$ ceramics measured in a magnetic field of 9.0 T between 5 K and 212 K. The quantities were calculated under the assumption that the concentration of the paramagnetic V ion equals 0.1 mol%.

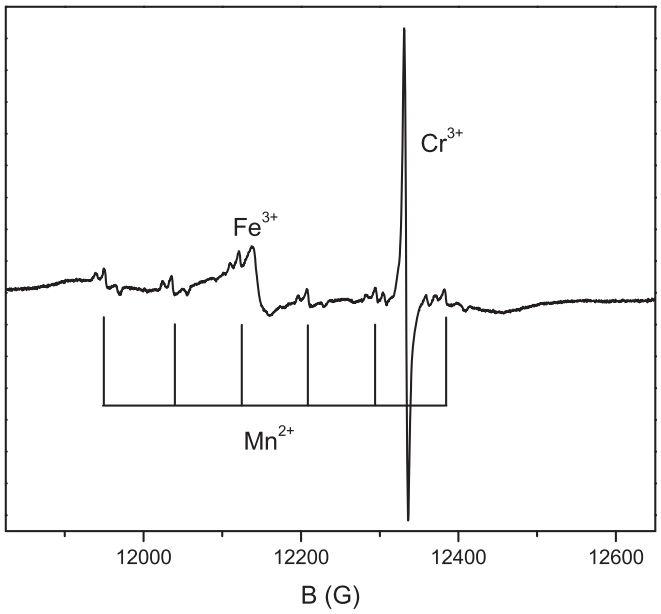

Figure 4. Room-temperature Q-band spectrum of the as-sintered 2 mol% V doped $BaTiO_3$ ceramics showing only the Cr^{3+}, Mn^{2+} and Fe^{3+} impurities of the samples without any signals corresponding to vanadium.

3.3. EPR measurements

3.3.1. As-sintered samples

In room-temperature spectra of our V-doped $BaTiO_3$ samples only the weak signals of Fe^{3+}, Cr^{3+} and Mn^{2+} ions are observed (see the Q-band spectrum in figure 4).

These impurity ions with concentrations less than 0.02 mol% stem from the source material TiO_2 [8, 10]. After cooling down the as-sintered samples (in air) to 6 K, additionally to the impurity lines a very broad line ($g \approx 1.96$, $\Delta B = 1600$ G) and peaks with low intensitity are observed in the X-band (figure 5), which can be clearly identified as the ^{51}V hyperfine splitting (HFS) octet of a vanadium spectrum. One of the HFS peaks is overlapping with a strong Fe^{3+} line (marked by an asterisk in figure 5).

Both, from the characteristic shape of the HFS peaks and from the different distances between two neighbouring peaks in the X-band spectrum (158 G in the low and 162 G in the high field, respectively), this spectrum can be identified as the parallel component of an axial spectrum. Due to the additional Fe^{3+} and Mn^{2+} lines in the centre of the spectrum the spectral resolution is rather low and the peaks of its perpendicular part are barely identifiable. This ^{51}V spectrum can be explained by the spin-Hamiltonian (1) with $S = 1/2$ and $I = 7/2$.

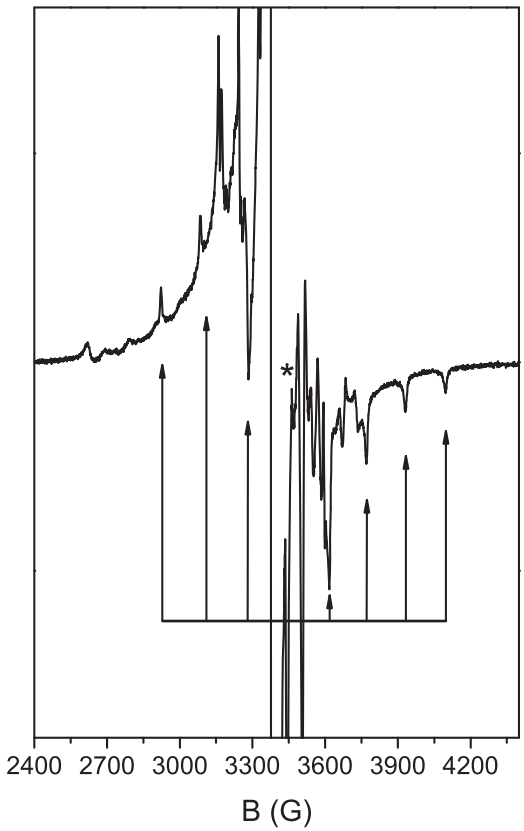

Figure 5. X-band spectrum of as-sintered 2 mol% V doped barium titanate ceramics, taken at 6 K. The broad line is superimposed by the strong signal (g = 2.0027) of Fe^{3+} ions and by a weak Mn^{2+} sextet. The HFS peaks of the parallel part of the V^{4+} powder spectrum are marked.

Table 1. Spin-Hamiltonian parameters of V^{2+} (S = 3/2) and V^{4+} (S = 1/2) in different oxide compounds.

	g	D (10^{-4} cm^{-1})	A (10^{-4} cm^{-1})
$BaTiO_3$:V^{2+}	1.9705(5)	280(20)	61(3)
cubic $SrTiO_3$:V^{2+} [22]	1.966	—	48.5
cubic MgO:V^{2+} [29]	1.991	—	79.4(3)
$BaTiO_3$:V^{4+}	1.930(1)[a]	—	150(5)[a]
$SrTiO_3$:V^{4+} [25]	1.9420(50)	—	146.78(5)

[a] = parallel component of the axial tensor

Its parameters were determined by simulation with the 'pepper' function of the Easy Spin packet [26] for MATLAB[1] and are given in table 1. Because of the electron spin S = 1/2 corresponding to a d^1 system, we assign this spectrum to V^{4+} ions, which is additionally supported by the values of spin-Hamiltonian parameters. Investigations in the Q-band show no improvement in resolution, since the V^{4+} signals are broadened by g-strain effects ($\Delta g_{||,\perp} \approx 0.0005$). Both the V^{4+} spectrum and the broad line are temperature-dependent. Their intensities decrease with temperature and above T = 20 K, they are no longer detectable.

3.3.2. Post-annealed samples

In the low-temperature X-band spectrum (T = 6 K) of the H_2/Ar-annealed samples the intensities of the V^{4+} spectrum and the broad line (see section 3.2.1) are increased in comparision with the air-sintered samples (see figure 6).

At temperatures higher than 20 K, the V^{4+} spectrum and the broad line vanish and a new powder pattern (centre of gravity g = 1.97, marked by asterisks) is well visible in the X-band spectrum at T = 35 K. To get a better disentanglement of the new pattern from the fine structure transitions of Mn^{2+}, Fe^{3+} and Cr^{3+} ions and to reduce second order effects, all further investigations were performed in the much higher magnetic field of a Q-band spectrometer at temperatures above T = 20 K. Figure 7 shows the Q-band spectrum at 35 K with the

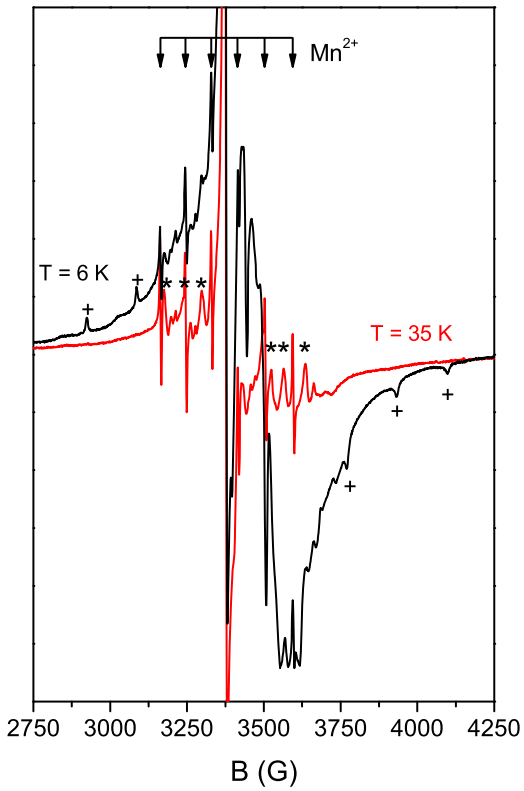

Figure 6. X-band spectrum of H_2/Ar-annealed 2 mol% V doped $BaTiO_3$ ceramics taken at 6 K and 35 K. In the 6 K spectrum, the V^{4+} lines are marked by plus signs (+). The V^{2+} pattern at T = 35 K is marked by asterisks (*). Both patterns are overlaid by Fe^{3+} and Mn^{2+} signals.

characteristic ^{51}V HFS octet expected for the nuclear spin of 7/2. Each of the eight peaks is split into two main components. The distance Δ between them (marked in the figure at the right-most HFS peak) is dependent on the microwave frequency of the experiment. In the Q-band spectrum, the average distance Δ is about 21.2 G. Furthermore, another feature is observed in this vanadium spectrum. At higher amplification, signals with very low intensity are visible between the pairs of HFS peaks, which are marked in figure 7 by asterisks. These two peculiarities are attributed to the fine structure splitting of the spectrum as described in the following.

V^{4+} (d^1, S = 1/2) can be easily excluded from the possible paramagnetic vanadium valence states 4+, 3+, 2+ corresponding to d^1 (S = 1/2), d^2 (S = 1) and d^3 (S = 3/2), respectively, because of the observed fine structure splitting. The V^{3+} ion with integral spin S = 1 can also be ruled out for the following reasons. First, the observed good resolution of the HFS octet in a powder spectrum is only possible in the case of a small fine structure parameter D, whereas for V^{3+} large D values of about 5 cm^{-1} have been reported [30, p. 427]. This large D would cause a strong angular dependence in the single-crystal rotation pattern and consequently their powder pattern has a completely other shape as observed in our experiment. Second, an integral spin would yield a considerably larger line width due to the increased spin-lattice coupling [31]. Hence, the observed spectrum is caused by V^{2+} with S = 3/2 and may be described by the spin-Hamiltonian with a fine structure term according to equation (2). In the spectrum (figure 7 a) only the HFS lines of the central transition are seen.

The feature of the powder pattern for a S = 3/2 spin-system (discussed in [7]) corresponds to the splitting Δ of the HFS lines (see figure 7) of the central fine structure transition $M_S = -\frac{1}{2} \leftrightarrow M_S = +\frac{1}{2}$ (M_s - electronic magnetic quantum number). The EPR line of this transition becomes weakly angular-dependent by effects of the off-diagonal elements in the spin-Hamiltonian matrix (2) giving small angular-dependent shift of its resonance field the order $D^2/(g\mu_B B)$. This effect results in a weak peak splitting of the central transition in the powder spectrum. Its magnitude is determined by the microwave frequency and the fine-structure parameter D. In addition to the peaks of the central transition lines according to the selection rules $M_S = \pm\frac{1}{2} \leftrightarrow M_S = \pm\frac{3}{2}$ are expected in the low- and high-field part of the powder spectrum. However, in our case these peaks could not be detected. We explain this effect by line broadenings arising by D-strain (characterized by the parameter ΔD) in the ceramic samples. Since the resonance fields of the transitions $M_S = \pm\frac{1}{2} \leftrightarrow M_S = \pm\frac{3}{2}$ are linearly dependent on D, the transitions broaden so strongly that their peaks are not observable in the spectra. Only the peaks of the central transition oft the V^{2+} spectrum can be detected because their line broadening are

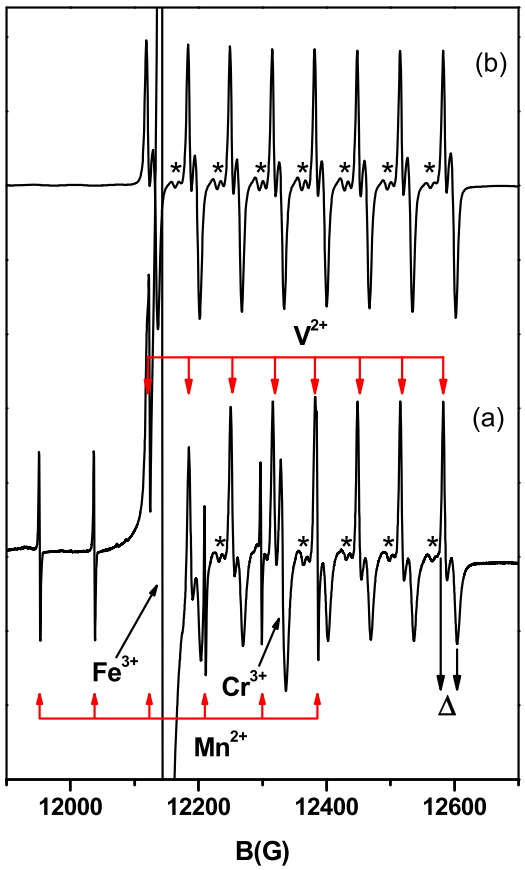

Figure 7. Q-band spectrum (T = 35 K) of H_2/Ar- annealed 2 mol% V doped $BaTiO_3$ ceramics (a) and the corresponding simulated spectrum with the allowed and forbidden ^{51}V HFS peaks of the central transition of the V^{2+} ions (b). For the simulation the spin-Hamiltonian parameters of the V^{2+} ion given in table 1 were used. The peaks of the forbidden HFS-transitions are marked by asterisks (*).

proportional to $\frac{D^2}{g\,\mu_B B} < \Delta D$. This is a specific characteristic of EPR spectra of Mn^{2+}-, Fe^{3+}- and Cr^{3+}- doped $BaTiO_3$-samples [8].

In the case of divalent vanadium ions with $3d^3$ configuration, the hyperfine interaction of the ^{51}V isotope yields a splitting of the central fine structure peak $M_S = -\frac{1}{2} \leftrightarrow M_S = +\frac{1}{2}$ in eight allowed peaks ($\Delta M_S = \pm 1$, $\Delta M_I = 0$, M_I - nuclear magnetic quantum number) and induces furthermore forbidden transitions with the selection rules $\Delta M_S = \pm 1, \Delta M_I = \pm 1$, lying between the allowed peaks of the central transition [30]. Such kind of transitions become detectable by second-order admixtures arising from the cross products of fine and hyperfine terms in equation (2). The intensity of these doublets $\left|\frac{1}{2}, M_I\right\rangle \leftrightarrow \left|-\frac{1}{2}, M_I + 1\right\rangle$ and $\left|\frac{1}{2}, M_I + 1\right\rangle \leftrightarrow \left|-\frac{1}{2}, M_I\right\rangle$ relative to the allowed ones $\left|\frac{1}{2}, M_I\right\rangle \leftrightarrow \left|-\frac{1}{2}, M_I\right\rangle$ (Dirac ket notation $|M_S, M_I\rangle$) was first given by Bleaney and Rubins [32] and can be written as

$$16(3D\sin 2\theta/4g\mu_B B)^2\,[I(I+1) - M_I(M_I - 1)]. \quad (3)$$

Therefore, their intensities allow the determination of the axial fine-structure parameter D if the fine-structure peaks with the selection rules $M_S = \pm\frac{1}{2} \leftrightarrow M_S = \pm\frac{3}{2}$ cannot be detected in the powder spectrum. The occurrence of forbidden peaks in the central fine-structure transition is an unequivocal proof of the existence of paramagnetic V^{2+} ions with a half-integral electron spin S = 3/2. Assuming the spin-Hamiltonian (2) with S = 3/2 for the explanation of the V^{2+}-powder-pattern, its parameters were evaluated by simulation and are given in table 1.

The simulated spectrum is shown in figure 7. At T = 35 K, the width of the individual lines is about (2.1 ± 0.2) G and ΔD of the fine-structure parameter distribution is estimated to be $(50 \pm 8) \cdot 10^{-4}$ cm^{-1}. Due to this high value of ΔD, the peaks belonging to the transitions $M_S = \pm\frac{1}{2} \leftrightarrow M_S = \pm\frac{3}{2}$ are broadened and cannot be detected in the experiment (figure 7).

In figure 8, the temperature dependence of the V^{2+} spectrum of the H_2/Ar-annealed sample is presented. Above T = 20 K, the peaks of V^{2+} centers are observed in the powder spectrum besides the lines of Mn^{2+}, Fe^{3+} and Cr^{3+} ions. Up to T = 170 K, the line widths and distances of V^{2+} peaks are nearly temperature independent.

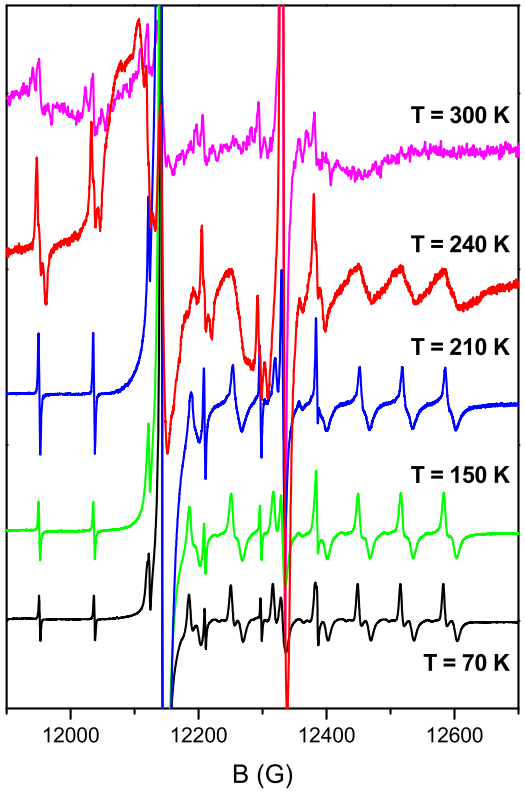

Figure 8. Temperature dependence of the V^{2+} spectrum of H_2/Ar-annealed 2 mol% V doped $BaTiO_3$ ceramics measured in the Q-band.

Only at higher temperatures the peaks broaden and their amplitudes decrease. By further increase of temperature the peak splittings are no longer resolved and nearly symmetric lines with small intensities are observed. Above 250 K the V^{2+} spectrum is no more detectable. The hyperfine constant A of the V^{2+} ion is nearly temperature-independent. The absence of the peaks belonging to the fine structure transitions $M_S = \pm\frac{1}{2} \leftrightarrow M_S = \pm\frac{3}{2}$ prevents the accurate measurement of the temperature dependence of the axial and rhombic fine structure parameters.

4. Discussion

Dependent on the position of the Fermi level in the band gap of barium titanate the 3d-element vanadium has different oxidation states and can be incorporated as diamagnetic ion V^{5+} (electron configuration $3d^0$, free ion ground state ^1S) as well as paramagnetic ions V^{4+} ($3d^1$, ^2D), V^{3+} ($3d^2$, ^3F) and V^{2+} ($3d^3$, ^4F). By incorporation of the impurity ion on the Ti^{4+} site vanadium is surrounded by six oxygen ions forming a distorted octahedron in the ferroelectric phases of the 3 C modification of $BaTiO_3$. However, in the paraelectric high-temperature phase the octahedron is regular. Owing to the strong local electrical field with octahedral symmetry the orbital degeneracy of the free-ion states is partially lifted [30]

$$^2D(V^{4+}) \rightarrow {}^2T_{2g}(V^{4+}) + {}^2E_g(V^{4+})$$
$$^3F(V^{3+}) \rightarrow {}^3T_{1g}(V^{3+}) + {}^3T_{2g}(V^{3+}) + {}^3A_{2g}(V^{3+})$$
$$^4F(V^{2+}) \rightarrow {}^4A_{2g}(V^{2+}) + {}^4T_{2g}(V^{2+}) + {}^4T_{1g}(V^{2+}).$$

Only in the case of V^{2+} ion, the ground state is a non-degenerate orbital state ($^4A_{2g}$) whose spin degeneracy can only be removed by the spin–orbit interaction in combination with the crystalline electrical field of lower symmetry. In contrast to V^{2+}, the tetra- and trivalent vanadium ions have triply orbital-degenerate ground states with the symmetries T_2 and T_1, respectively. According to the Jahn-Teller (JT) theorem such ground states are unstable and their degeneracy is lifted e.g. by small displacements of the neighbouring ions, which lower the symmetry of the crystal field. Since ions with the electronic ground state $^3A_{2g}$ have a long spin-lattice relaxation time [30] V^{2+} ions should be detected by EPR up to room temperature in contrast to ions with T ground states, which are principally not observable at RT by EPR.

On the basis of the observed hyperfine splitting, the resolved vanadium spectrum detected in the as-sintered $BaTiO_3$ powder samples was attributed to V^{4+} ions with $S = 1/2$ substituting for Ti^{4+}. The orbital degeneracy of its ground state is lifted by a Jahn-Teller effect between the electronic state T_{2g} of the V^{4+} and a localized vibronic e_g mode in the linear coupling case. This static Jahn-Teller effect produces an axial distortion of the oxygen octahedron in which the paramagnetic V^{4+} is incorporated. This symmetry reduction is reflected in the axially symmetric spin-Hamiltonian for V^{4+}. The same situation has been observed for other impurities with $3d^1$ electron configuration in $BaTiO_3$ and $SrTiO_3$ [24, 33, 34]. The EPMA measurement revealed that only about 0.1 mol% V is incorporated in the grains. Hence, the concentration of V^{4+} is probably even lower, since the presence of V^{5+} is very likely (see below). In the as-sintered samples EPR spectra of divalent vanadium were not obseserved.

After post-annealing in H_2/Ar atmosphere the charge state of the vanadium ions is partially changed and a new EPR spectrum is observed. Based on the distinctive feature of this spectrum it has to be assigned to V^{2+} ions with the electron spin $S = 3/2$ located at Ti^{4+} sites. In the rhombohedral and orthorhombic modifications of $BaTiO_3$ the symmetry of the Ti^{4+} lattice site is lower than the tetragonal one and a spectrum with orthorhombic symmetry is expected. Due to the lack of outer peaks of the transitions with selection rules $M_S = \pm\frac{3}{2} \leftrightarrow M_S = \pm\frac{1}{2}$ the local symmetry of the V^{2+} site cannot be determined unambiguously. The simulation of the V^{2+} spectra using the spin-Hamiltonian (2) augmented by the orthorhombic term $E(S_x^2 - S_y^2)$ illustrates additional splittings in the central peaks if $E > 25{\cdot}10^{-4}$ cm^{-1}. Therefore, a small orthorhombic distortion of V^{2+} spectrum cannot be excluded. At 35 K, the axial zero field splitting parameter D of V^{2+} is in very good accordance with the value of the Cr^{3+} ion having the same ground state as V^{2+} [35]. The ^{51}V HFS constant A of $61{\cdot}10^{-4}$ cm^{-1} is smaller than the value of V^{2+} ions in the ionic crystal MgO (see table 1). This reduction can be attributed to the delocalisation of the unpaired V^{2+} electrons onto orbitals of the Ti-O states.

V^{2+} ions with the electronic ground state $^4A_{2g}$ have a long spin-lattice relaxation time. Their spectra should be easily detected at and above room temperature as observed for other d^3 ions, see e.g. [7, 35–37]. However, with increasing temperature, in our samples a line width broadening of the V^{2+} spectrum appears above 210 K and finally the spectrum vanishes at $T > 240$ K. Due to the complexity of the observed peak structure it is not possible to determine the individual line width as a function of temperature. It can be assumed that the temperature-dependent line width broadening and finally the complete disappearance of the spectrum is caused by a thermally activated charge carrier transfer process between V^{2+} and V^{3+} states (see below).

The presence of the other possible valence states V^{5+} and V^{3+} in the $BaTiO_3$ grains can be concluded by following consideration. The samples annealed in reducing atmosphere show an increased intensity of the V^{4+} spectrum i.e. an increased concentration of V^{4+} ions. This indicates that a part of the V^{5+} in the as-sintered $BaTiO_3$ grains is reduced to V^{4+} during annealing. Moreover, since the reduced samples include both V^{4+} and V^{2+} ions, it is possible that also V^{3+} ions (d^2, $S = 1$) occur in those samples, which are not detected by our EPR experiments.

In the spectra of all V-doped $BaTiO_3$ samples a broad line was observed up to 20 K. Because of the sparse spectral information its interpretation is difficult. We suppose that this line is caused by V^{4+} ions in the vanadium-rich secondary phase containing practically the whole V dopant (see section 3.3.1). Due to the higher concentration of the V^{4+} ions (see discussion of the magnetic susceptibility below) they are coupled by dipole-dipole-interaction and only a single broad line is observed.

The very small paramagnetic susceptibility of the as-sintered samples (figure 3) proves that the majority of vanadium in the secondary phases (95% of the dopant amount) is in the valence state 5+. The measured magnetic moment is a superposition of the contribution of the V^{4+} ions both in the $BaTiO_3$ grains and in the vanadium-rich $Ba_3V_2O_8$ phase, proven by XPS [28]. Since the experimental determined value of the effective Bohr magneton number is very uncertain because of the unknown concentration of V^{4+} and since the spin-only formula is not suitable for ions with T_{2g} ground state as V^{4+}, the computer program CONCORD [38] was used for the analysis of the susceptibility data. Simulations of the temperature dependence of the molar magnetic susceptibility showed that the measured data can only be reasonably reproduced if either a lower-symmetric than octahedral or a tetrahedral crystal field is assumed. Both variants occur in the samples, first as tetragonally JT-distorted oxygen octahedra in the $BaTiO_3$ grains and second as VO_4-tetrahedra around the vanadium ions in the crystal structure of $Ba_3V_2O_8$ (space group $R\bar{3}m$) [39]. Since less than 0.1 mol% of V^{4+} is incorporated in the $BaTiO_3$ grains, we assume that the majority of V^{4+} is located in the $Ba_3V_2O_8$ phase and in turn the tetrahedrally oxygen coordinated V^{4+} ions dominate the paramagnetic susceptibility. Thus, the susceptibility data were fitted by CONCORD (for details see appendix A of [9]) assuming a crystal field with symmetry T_d and including the concentration of the paramagnetic ions as a further fitting parameter. The total concentration of the V^{4+} ions was found to be 0.6 mol% confirming our assumption *a posteriori*. The crystal field fitting parameter[7] B_0^4 amounts to ≈ -1000 cm^{-1}.

[7] Wybourne notation [40].

5. Conclusions

Vanadium exhibits a very low solubility of about 0.1 mol% in the $BaTiO_3$ grains of nominally 2.0 mol% V doped ceramics sintered in air at 1400 °C. The majority of vanadium (95%) forms the secondary phase $Ba_3(V/Ti)_2O_8$. Up to a nominal doping concentration of 10 mol% V the solubility in $BaTiO_3$ remains below 0.2 mol%. This low V content is probably the reason that all samples investigated (both as-sintered and post-annealed in reducing atmosphere) are completely in tetragonal phase at RT whereas the other 3d ions Cr–Zn cause at least the partial formation of the hexagonal phase already at nominal doping concentrations of 0.5 mol%.

In the as-sintered samples, V occurs in V^{4+} and V^{5+} valence state. The former was detected with EPR by its HFS octet due to the nuclear spin of 7/2 of ^{51}V and was identified as V^{4+} ions incorporated at the Ti^{4+} site of $BaTiO_3$. As a second species V^{4+} was found in the V-rich secondary phase $Ba_3(V/Ti)_2O_8$ as a single broad line. In the samples post-annealed in reducing atmosphere, an additional HFS octet occurs, which can be assigned unambiguously to V^{2+} ions with a half-integer electron spin of 3/2 by the occurrence of both allowed and forbidden fine structure transitions.

ORCID iDs

H T Langhammer https://orcid.org/0000-0003-2603-093X
S G Ebbinghaus https://orcid.org/0000-0001-6391-2582

References

[1] Moulson A J and Herbert J M 2003 *Electroceramics: Materials, Properties, Applications* (New York: Wiley)
[2] Chen Y L and Yang S F 2011 *Adv. Appl. Ceramics* **110** 257
[3] Acosta M, Novak N, Rojas V, Patel S, Vaish R, Koruza J, Rossetti G A Jr and Rödel J 2017 *Applied Physics Reviews* **4** 041305
[4] Keith G M, Rampling M J, Sarma K, Alford N M and Sinclair D C 2004 *J. Euro. Ceram. Soc.* **24** 1721
[5] Jayanthi S and Kutty T R N 2008 *J. Mater. Sci.: Mater. Electron.* **19** 615
[6] Müller K A and Kool T W 2010 *Properties of Perovskites and Other Oxides* (Singapore: World Scientific)
[7] Böttcher R, Erdem E, Langhammer H T, Müller T and Abicht H-P 2005 *J. Phys.: Condens. Matter* **17** 2763
[8] Böttcher R, Langhammer H T, Kücker S, Eisenschmidt C and Ebbinghaus S G 2018 *J. Phys.: Condens. Matter* **30** 425701
[9] Langhammer H T, Böttcher R, Müller T, Walther T and Ebbinghaus S G 2015 *J. Phys.: Condens. Matter* **27** 295901
[10] Böttcher R, Langhammer H T and Müller T 2011 *J. Phys.: Condens. Matter* **23** 115903
[11] Langhammer H T, Müller T, Böttcher R and Abicht H-P 2003 *Solid State Sci.* **5** 965
[12] Feltz A and Langbein H 1971 *Kristall und Technik* **6** 359
[13] Ihrig H 1978 *J. Phys. C: Solid State Physics* **11** 819
[14] Hagemann H-J 1980 Acceptor ions in $BaTiO_3$ and $SrTiO_3$ and their consequences on the properties of titanate ceramics *Ph. D. thesis* (RWTH Aachen)
[15] Schwartz R N and Wechsler B A 1993 *Phys. Rev.* B **48** 7057
[16] Liu S, Zenou V Y, Sus I, Kotani T, van Schilfgaarde M and Newman N 2007 *Acta Mater.* **55** 2647
[17] Cai W, Fu C, Lin Z and Deng X 2011 *Ceramics International* **37** 3643
[18] Stanuch K 2014 *Technical Transactions (Chemistry)* **111** 109
[19] Dulian P, Bak W, Wieczorek-Ciurowa K and Kajtoch C 2014 *Materials Science - Poland* **32** 257
[20] Moura F, Simoes A Z, Cavalcante L S, Zaghete M A, Varela J A and Longo E 2008 *Journal of Alloys and Compounds* **466** L15
[21] Fu C, Liang J, Cai W, Chen G and Deng X 2013 *J. Mater. Sci.: Mater. Electron.* **24** 2438
[22] Müller K A, Aguilar M, Berlinger W and Blazey K W 1990 *J. Phys.: Condens. Matter* **2** 2735
[23] Shibahara T, Yonezawa Y, Satoh J, Kido O and Natsui H 2011 *Jap. J. Appl. Phys.* **50** 09NC12
[24] Kool T W and Glasbeek M 1991 *J. Phys.: Condens. Matter* **3** 9747
[25] Kool T W and Glasbeek M 1979 *Sol. State Comm.* **32** 1099
[26] Stoll S and Schweiger A 2006 *J. Magn. Reson.* **178** 42
[27] Reed S J B 1993 *Electron microprobe analysis* 2nd Ed (Cambridge: Cambridge University Press) p 199
[28] Guo D, Hu C and Xi Y 2013 *J. Alloys Compd.* **550** 389
[29] Low W 1956 *Phys. Rev.* **101** 1827
[30] Abragam A and Bleany B 1970 *Electron Paramagnetic Resonance of Transition Ions* (Oxford: Clarendon)
[31] Pake G E and Estle T L 1973 *Electron and Paramagnetic Resonance (Frontiers in Physics)* 2nd edn (New York: Benjamin)
[32] Bleaney B and Rubins R S 1961 *Proc. Phys. Soc.* **77** 103
[33] de Jong H J and Glasbeck M 1976 *Solid State Commun.* **19** 1197
[34] de Jong H J and Glasbeck M 1978 *Solid State Commun.* **28** 683
[35] Müller K A, Berlinger W and Albers J 1985 *Phys. Rev.* B **32** 5837
[36] Blazey K W, Cabrera J M and Müller K A 1983 *Sol. St. Comm.* **45** 903
[37] Böttcher R, Langhammer H T, Müller T and Abicht H P 2005 *J. Phys.: Condens. Matter* **17** 4925
[38] Schilder H 2015 Programm CONCORD, Fachhochschule Aachen http://condon.fh-aachen.de
[39] Süsse P and Buerger J 1970 *Z. Kristallogr.* **131** 161
[40] Wybourne B G 1965 *Spectroscopic Properties of Rare Earths* (New York: Wiley)